Adaptive Noise Estimation for Homing Missiles

David G. Hull* and Jason L. Speyer*
The University of Texas, Austin, Texas
and
William M. Greenwell†
McDonnell-Douglas Technical Service Company, Houston, Texas

The presence of a microprocessor makes it possible to utilize a digital filter to process the measurement data and obtain a state estimate to be used in a digital guidance system for tactical homing missiles. Of particular interest is the case of the short-range, air-to-air missile against a highly maneuverable target when angle-only measurements are available. A standard filter for processing the measurements is the extended Kalman filter, the performance of which depends on the value selected for the measurement covariance. It is shown that the performance of this filter can be improved by estimating the measurement covariance. Two methods for doing so are investigated: the limited-memory and the weighted limited-memory.

Nomenclature

B = convolution integral
H = $\partial h(x)/\partial x$
h = measurement-state function
K = Kalman gain
M = a priori error covariance
N = number of samples in window
P = error covariance
Q = process noise power spectral density
q = measurement noise power spectral density
r = residual
V = measurement noise covariance
v = measurement noise
$\bar{v}$ = sample mean of N residuals
w = process noise
x,y,z = inertial components
x = state vector
$\bar{x}$ = a priori state estimate
$\hat{x}$ = state estimate
z = measurement vector
β = integer delaying use of noise samples in weighted limited-memory filter (WLMF)
λ_T = target maneuver time constant
σ = ratio of actual noise variance to filter noise variance
Φ = transition matrix
ω = weight factor in WLMF

Subscripts

r = relative
θ = azimuth
ϕ = elevation

Introduction

RECENT advances in microprocessor technology make practical the use of digital guidance systems that can implement sophisticated estimation functions. An estimation scheme is described herein that improves the miss performance relative to previous designs for short-range, air-to-air missiles against highly maneuverable targets when only the angle measurements are available. The guidance loop is depicted in Fig. 1 where the plant includes the missile and target dynamics and relative geometry. The digital guidance system is composed of a nonlinear filter, called the extended Kalman filter (EKF), followed in cascade by the guidance scheme formed by a set of gains operating linearly on the filter outputs. The computation associated with the EKF[1] is increased over fixed-gain filters since the approximate error variance associated with the state estimate, and thereby the filter gains, is computed on line. The control gains, if calculated from linear-quadratic-Gaussian (LQG) theory,[2] are functions of only time-to-go.

The miss distance produced by this guidance system is very sensitive to the values of the measurement noise variance.[3] Unfortunately, the measurement noise variance is not known a priori. A scheme for estimating the measurement noise variance using the residuals from the EKF has been developed[4] and shown to improve the miss distance performance. The approximate error variance and, thereby, the Kalman filter gains adapt to the on-line estimated value of the measurement variance.

First, the engagement model used for the filter and guidance formulation is presented. Then, the EKF algorithm for estimating the measurement variance from a small sample of residuals from the EKF over a fixed interval is discussed. Finally, the six degree-of-freedom bank-to-turn simulation is described, and the simulation results demonstrating the miss performance of the adaptive estimation schemes are given and compared with the nonadaptive scheme.

System Model for Filter/Guidance Law Derivations

The system dynamics and measurement process used to derive the filter and guidance law are simplified by the assumptions that the missile acceleration is measured very accurately by accelerometers and that the autopilot dynamics are neglectable. The equations of relative inertial motion between the missile and target are given by the linear kinematic equations

$$\dot{S}_r = V_r, \qquad \dot{V}_r = A_T - A_M \tag{1}$$

where the engagement geometry is shown in Fig. 2. In these equations, S_r is the relative position vector, V_r the relative

Presented as Paper 82-1507 at the AIAA Guidance and Control Conference, San Diego, Calif., Aug. 9-11, 1982; submitted Aug. 18, 1982; revision received July 18, 1983.

*Professor, Department of Aerospace Engineering and Engineering Mechanics.
†Senior Engineer.

velocity vector, A_T the target acceleration vector, and A_M the missile acceleration vector. The target acceleration is modeled as the first-order Gauss-Markov process

$$\dot{A}_T = -\lambda_T A_T + w_T \tag{2}$$

where λ_T is the target maneuver time constant and w_T the maneuver uncertainty (Gaussian white noise with a zero mean and a power spectral density q_T). The parameters λ_T and q_T are chosen so that the autocorrelation function for a Poisson process for some given average switch time λ_T and maximum acceleration is the same as the autocorrelation function for this Gauss-Markov process.

In rectangular coordinates relative to an inertial reference frame, the scalar components of the above quantities are given by (see Fig. 2)

$$\begin{aligned} S_r^T &= [x_r y_r z_r] & V_r^T &= [\dot{x}_r \dot{y}_r \dot{z}_r] \\ A_T^T &= [a_{T_x} a_{T_y} a_{T_z}] & A_M^T &= [a_{M_x} a_{M_y} a_{M_z}] \\ w_T^T &= [w_{T_x} w_{T_y} w_{T_z}] \end{aligned} \tag{3}$$

In terms of the nine-component state vector

$$x^T = [x_r y_r z_r \dot{x}_r \dot{y}_r \dot{z}_r a_{T_x} a_{T_y} a_{T_z}] \tag{4}$$

the dynamics of the system are defined by the linear equation

$$\dot{x} = Fx + GA_M + w \tag{5}$$

where, if I_3 is the 3×3 identity matrix and 0_3 the 3×3 null matrix,

$$F = \begin{bmatrix} 0_3 & I_3 & 0_3 \\ 0_3 & 0_3 & I_3 \\ 0_3 & 0_3 & -\lambda_T I_3 \end{bmatrix} \qquad \begin{aligned} G^T &= [0_3 - I_3 0_3] \\ w^T &= [0_3 0_3 w_T^T] \end{aligned} \tag{6}$$

For angle-only measurements, the nonlinear measurement-state relations are given by

$$z_\theta = \theta + v_\theta, \qquad z_\phi = \phi + v_\phi \tag{7}$$

where

$$\begin{aligned} \theta &= h_\theta(x) \triangleq \tan^{-1}(y_r/x_r) \\ \phi &= h_\phi(x) \triangleq \tan^{-1}[z_r/(x_r^2+y_r^2)^{1/2}] \end{aligned} \tag{8}$$

The random sequences v_θ and v_ϕ represent independent noise sources with zero means and the following variances:

$$V_{\theta\theta} = q_\theta/\Delta t, \qquad V_{\phi\phi} = q_\phi/\Delta t \tag{9}$$

where Δt is the sample period. The power spectral densities q_θ and q_ϕ are modeled as

$$\begin{aligned} q_\theta &= q_{-1,\theta}/R^2 + q_{0,\theta} \\ q_\phi &= q_{-1,\phi}/R^2 + q_{0,\phi} \end{aligned} \tag{10}$$

where R is the range and the remaining parameters are assumed known. The adaptive feature, to be described later, estimates $V_{\theta\theta}$ and $V_{\phi\phi}$ on line.

In general terms, the measurement vector is $z \triangleq [z_\theta z_\phi]^T$, the measurement vector function is $h(x) \triangleq [h_\theta(x) h_\phi(x)]^T$, and the measurement noise vector is $v \triangleq [v_\theta v_\phi]^T$. Therefore, at time t_i where $x_i = x(t_i)$, Eq. (7) is rewritten as

$$z_i = h(x_i) + v_i \tag{11}$$

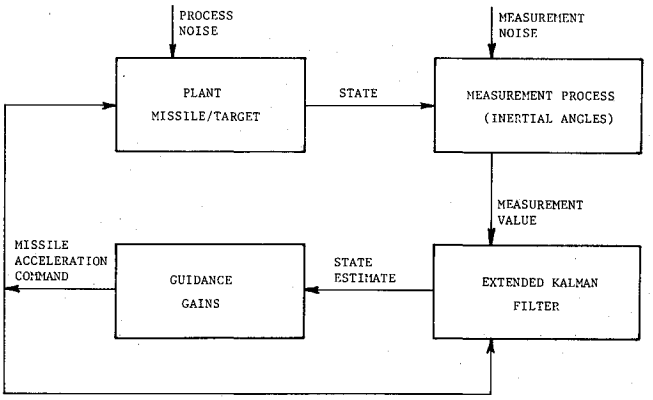

Fig. 1 Guidance loop.

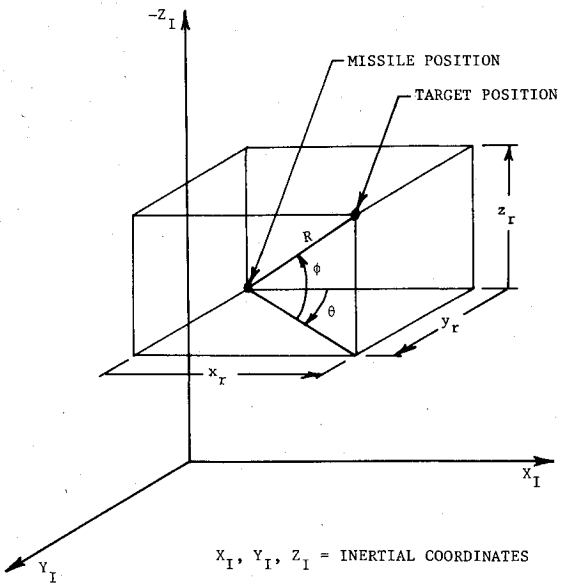

Fig. 2 Intercept geometry and measurement angles.

The zero-mean, independent noise sequence v_i has variance $V(t_i)$ with only the diagonal elements given by Eq. (9) being nonzero.

The EKF described in the next section is formulated in discrete time. Therefore, the discrete form of Eq. (5) is required. Since F and G in Eq. (6) are sufficiently elementary, the required transition matrix Φ and convolution integral B are obtained in closed form as

$$\Phi = \begin{bmatrix} I_3 & (\Delta t) I_3 & \dfrac{1}{\lambda_T^2}(e^{-\lambda_T \Delta t} + \lambda_T \Delta t - 1) I_3 \\ 0_3 & I_3 & \left(\dfrac{1}{\lambda_T} - \dfrac{1}{\lambda_T} e^{-\lambda_T \Delta t}\right) I_3 \\ 0_3 & 0_3 & (e^{-\lambda_T \Delta t}) I_3 \end{bmatrix}$$

$$B = \{[-(\Delta t)^2/2] I_3, \quad (\Delta t) I_3, \quad 0_3\}^T \tag{12}$$

Here, Φ and B are dependent on the sample interval Δt but not on the sample time t_i, i.e., $\Phi = \Phi(\Delta t)$ and $B = B(\Delta t)$. The discrete form of the equations of motion is

$$x_{i+1} = \Phi x_i + B A_{Mi} + w_{di} \tag{13}$$

where the w_{di} is the discrete form of the white process noise having zero mean and covariance

$$E[w_{di}w_{dj}^T]=0, \qquad i\neq j$$
$$\triangleq W, \qquad i=j \tag{14}$$

where

$$W=\int_{t_i}^{t_{i+1}} \Phi(t_{i+1}-\tau)GQG^T\Phi^T(t_{i+1}-\tau)\,d\tau,$$

and Q is the power spectral density of w in Eq. (6) where only the last three elements along the diagonal are nonzero and equal to q_T.

The Extended Kalman Filter

The extended Kalman filter (EKF) is an ad hoc nonlinear filter based on the rigorous results of the Kalman filter for linear systems. The essential feature of the EKF is that the assumed linearization is performed about the present estimate of the state. Therefore, the associated approximate error variance must be calculated on line so as to compute the EKF gains. Let the EKF a posteriori estimate at time t_i, given the measurement history $Z_i=\{z_1,\ldots,z_i\}$, be denoted as $\hat{x}_i$ and the approximate a posteriori error variance at t_i given Z_i be denoted as P_i. Fortunately, since the engagement dynamic model [Eq. (13)] is linear, the a priori estimate $\bar{x}_{i+1}$ given Z_i and the a priori approximate error variance M_{i+1} are given by

$$\bar{x}_{i+1}=\Phi\hat{x}_i+BA_{Mi} \tag{15}$$

$$M_{i+1}=\Phi P_i\Phi^T+W \tag{16}$$

At each measurement time the estimate and approximate error variance are updated as

$$\hat{x}_i=\bar{x}_i+K_i[z_i-h(\bar{x}_i)] \tag{17}$$

$$P_i=M_i-K_iH_iM_i \tag{18}$$

where the EKF gain is

$$K_i=M_iH_i^T[H_iM_iH_i^T+V_i]^{-1} \tag{19}$$

In these equations,

$$H_i\triangleq\left[\frac{\partial h(x)}{\partial x}\right]_{x=\bar{x}_i} \tag{20}$$

that is, H_i is a 2×9 matrix of the partial derivatives of h with respect to x evaluated at $\bar{x}_i$. This linearization about $\bar{x}_i$ is the approximation that leads to the extended form of the Kalman filter and the requirement that the approximate error variances [Eqs. (16) and (18)] must be propagated on line.

The residual process, the difference between the measurement and the predicted measurement, is

$$r_i\triangleq z_i-h(\bar{x}_i) \tag{21}$$

In the Kalman filter, the residuals can be shown to be a white, zero-mean process. For the EKF formulation, this process, known as the innovations process, is *assumed* to be an independent noise sequence with variance

$$E[r_ir_j^T]\cong 0 \qquad \text{if} \quad i\neq j$$
$$\cong V_i+H_iM_iH_i^T \qquad \text{if} \quad i=j \tag{22}$$

so that statistical small sampling theory, described in the next section, is applicable.

Adaptive Noise Estimation

The exact noise statistics required in an optimal Kalman filter are unknown in many applications. In particular, the characteristics of the measurement noise process for a homing missile are affected by unknown random disturbances in the sensor elements, atmospheric fluctuations, electronic jamming emitted from the target or some other source, and nonlinearities in the filter itself. Thus, in a real-time missile intercept, where the noise statistics generally exhibit nonstationary behavior, it is desirable to employ an adaptive, online noise estimator. In this section, the empirically obtained measurement residual sequence is used to estimate the statistics of the unknown noise distribution. The estimator discussed here is the limited-memory scheme derived in Ref. 4 that utilizes a sliding window to incorporate the most recent noise samples and to discard past samples. A modification whereby the residuals are age weighted is also considered.

Limited-Memory Noise Estimator

By using statistical sampling theory, the population mean and covariance of the residuals r_i formed in the EKF can be estimated by a sample mean and a sample covariance. Suppose a sample size of N is chosen; then the unbiased sample variance of the residuals is

$$\bar{C}_r=\frac{1}{N-1}\sum_{k=1}^{N}(r_k-\bar{v})(r_k-\bar{v})^T \tag{23}$$

where $\bar{v}$ is the sample mean of the residuals given by

$$\bar{v}=\frac{1}{N}\sum_{k=1}^{N}r_k \tag{24}$$

If the average value of HMH^T over the sample window is given by

$$\frac{1}{N}\sum_{k=1}^{N}H_kM_kH_k^T$$

Eqs. (22) and (23) lead to the following sample variance of the measurements at time t_N:

$$V=\frac{1}{N-1}\sum_{k=1}^{N}\left\{(r_k-\bar{v})(r_k-\bar{v})^T-\frac{N-1}{N}H_kM_kH_k^T\right\} \tag{25}$$

Recursion relations for the sample mean and sample covariance for $i>N$ can be formed as

$$\bar{v}_i=\bar{v}_{i-1}+\frac{1}{N}[r_i-r_{i-N}] \tag{26}$$

$$V_i=V_{i-1}+\frac{1}{N-1}\left\{(r_i-\bar{v}_i)(r_i-\bar{v}_i)^T\right.$$
$$-(r_{i-N}-\bar{v}_{i-N})(r_{i-N}-\bar{v}_{i-N})^T+\frac{1}{N}(r_i-r_{i-N})(r_i-r_{i-N})^T$$
$$\left.-\frac{N-1}{N}[H_iM_iH_i^T-H_{i-N}M_{i-N}H_{i-N}^T]\right\} \tag{27}$$

The sample mean computed by the adaptive scheme is a bias that must be accounted for in the Kalman filter algorithm. Therefore, the update equation (17) for the estimate becomes

$$\hat{x}_i=\bar{x}_i+K_i[z_i-h(\bar{x}_i)-\bar{v}_i] \tag{28}$$

Equations (24) and (25) are used to initialize this method after the first N samples of r_i and $H_iM_iH_i^T$ have been stored. Prior to the buildup of the sample window, the adaptive filter behaves as the unmodified extended Kalman filter using the

assumed a priori values of the measurement noise variance. At the sample time immediately following the initial adaptive estimate, the filter begins using the recursion relations given by Eqs. (26) and (27). These relations maintain the window size of N samples by throwing out the $(i-N)$th sample when the ith sample is included. This sliding window effect allows the filter to sense the time varying nature of the noise statistics. The window size N is a parameter to be determined through numerical experimentation.

Weighted Limited-Memory Noise Estimator

One method of gradually increasing the influence of the individual noise samples used in the adaptive filter is to multiply each one by a growing weight factor ω_i. The reasoning behind this approach is that the most recent noise samples are assumed to be more representative of the true distribution. In the missile intercept problem especially, the measurement residuals after a target maneuver occurs provide a better indication of the error in the filter prediction and should be weighted more heavily. In this analysis ω_i is generated by

$$\omega_i = (i-1)(i-2)\ldots(i-\beta)/i^{\beta} \tag{29}$$

where ω_i is the weight factor on the ith noise sample and β an integer that serves to delay the use of the noise samples. Notice that $\omega_i = 0$ for $i = 1,\ldots,\beta$ and that

$$\lim_{i\to\infty} \omega_i = 1$$

Thus, the weight factor begins as a small positive number after the βth sample and increases toward the limiting value of unity. The value of the parameter β is to be determined through numerical experimentation.

The weighted adaptive noise estimator is similar in form to the basic adaptive estimator. The sample mean at time t_N is initialized in batch form by

$$\bar{v}_i = \frac{1}{N}\sum_{k=1}^{N} \omega_k r_k \tag{30}$$

The sample mean is no longer unbiased, but it approaches an unbiased estimator asymptotically as ω approaches unity. The sample variance is initialized in batch form by

$$V = \frac{1}{N-1}\sum_{k=1}^{N}\left\{(\omega_k r_k - \bar{v})(\omega_k r_k - \bar{v})^T - \left(\frac{N-1}{N}\right)\omega_k^2 H_k M_k H_k^T - \left(\omega_k - \frac{\Omega}{N}\right)^2 [r_k r_k^T - H_k M_k H_k^T]\right\} \tag{31}$$

where

$$\Omega = \sum_{k=1}^{N} \omega_k$$

This estimator is also biased until ω approaches unity. As before, recursion relations, to be implemented after the initial estimate, are determined as

$$\bar{v}_i = \bar{v}_{i-1} + \frac{1}{N}[\omega_i r_i - \omega_{i-N} r_{i-N}] \tag{32}$$

Table 1 Launch conditions

Missile and target Mach number	0.9
Altitude	10,000 ft
Range	6,000 ft
Boresight	0 deg
Aspect angle	60 deg

$$V_i = V_{i-N} + \frac{1}{N-1}\left\{(\omega_i r_i - \bar{v}_i)(\omega_i r_i - \bar{v}_i)^T - (\omega_{i-N} r_{i-N} - \bar{v}_i)(\omega_{i-N} r_{i-N} - \bar{v}_i)^T + \frac{1}{N}(\omega_i r_i - \omega_{i-N} r_{i-N})(\omega_i r_i - \omega_{i-N} r_{i-N})^T + \frac{N-1}{N}[\omega_{i-N}^2 H_{i-N} M_{i-N} H_{i-N}^T - \omega_i^2 H_i M_i H_i^T] - \left(\omega_i - \frac{\Omega_i}{N}\right)^2 [r_i r_i^T - H_i M_i H_i^T] + \left(\omega_{i-N} - \frac{\Omega_i}{N}\right)^2 [r_{i-N} r_{i-N}^T - H_{i-N} M_{i-N} H_{i-N}^T]\right\} \tag{33}$$

where $\Omega_i = \Omega_{i-1} + (\omega_i - \omega_{i-N})$.

Additional computer storage and computational cost are introduced by these relations since the weighted noise samples $\omega_i r_i$ and $\omega_i^2 H_i M_i H_i^T$ must be stored and shifted as well as the noise samples r_i and $H_i M_i H_i^T$. Also, the weight factors must be computed, stored, and shifted. The improvement in filter performance relative to the increased storage and computational requirements can be determined only by computer simulation.

Computer Simulation

A six-degree-of-freedom missile simulation[5] has been used to test both of the adaptive noise estimators. This simulation contains the intercept of a maneuvering target by a short-range, air-to-air missile. The airframe aerodynamics and the autopilot of a bank-to-turn missile are included in the simulation as well as the digital filter and the guidance system. Each is a separate component capable of being modified without changing the rest of the program. The adaptive filters can be added to the extended Kalman filter in a straightforward manner.

An engagement begins with the firing of the missile from a launch aircraft that provides the relative position and velocity of the target. The target is assumed to be a constant-speed point mass that can change acceleration direction instantaneously. Initially, the target flies straight and level at the launch altitude. When the missile reaches a range of 6000 ft, the target commences a 9 g maneuver 45 deg up and to the right relative to its original heading. When the estimated time-to-go reaches 1 s, the target rolls 180 deg and pulls 9 g. The missile itself is capable of 100 g normal acceleration. An engagement ends when the closing velocity becomes negative or when a preset time limit is exceeded.

The actual measurement variance is obtained by multiplying $V_{\theta\theta}$ and $V_{\phi\phi}$ given in Eq. (9) by a parameter σ, which is called the mismatch parameter, allowing the true variance to be of a different order of magnitude than the value assumed in the filter. The value used in Eq. (10) for $q_{-1,\theta} = q_{-1,\phi}$ is 0.25 rad$^2 \cdot$ ft$^2 \cdot$ s, and the value for $q_{0,\theta} = q_{0,\phi}$ is 56.25×10^{-8} rad$^2 \cdot$ s. Finally, the sample time is $\Delta t = 0.02$, and $\lambda_T = 1\ \text{s}^{-1}$.

The launch conditions are the same for all simulations performed in this study and are given in Table 1. An initial range of 6000 ft has been chosen so the target is maneuvering throughout the entire engagement. The filter inputs that remain unchanged are the initial state estimate,

$$\hat{x}_r, \hat{y}_r, \hat{z}_r = \text{true value, ft}$$

$$\hat{\dot{x}}_r, \hat{\dot{y}}_r, \hat{\dot{z}}_r = \text{true value, ft/s}$$

$$\hat{a}_{T_x} = \hat{a}_{T_y} = \hat{a}_{T_z} = 0\ \text{ft/s}^2 \tag{34}$$

the a priori, diagonal, covariance matrix M_0, which introduces uncertainty in the initial conditions,

$$M_0(1,1) = M_0(2,2) = M_0(3,3) = 10 \text{ ft}^2$$

$$M_0(4,4) = M_0(5,5) = M_0(6,6) = 10 \text{ ft}^2/\text{s}^2$$

$$M_0(7,7) = M_0(8,8) = M_0(9,9) = 25{,}000 \text{ ft}^2/\text{s}^4 \quad (35)$$

and the process noise spectral density matrix Q

$$Q(7,7) = Q(8,8) = Q(9,9) = 50{,}000 \text{ ft}^2\text{s}^5 \quad (36)$$

Adaptive Filter Testing

The limited-memory filter (LMF) and the weighted limited-memory filter (WLMF) are compared with the extended Kalman filter (EKF) for nine different cases representing three values of the noise mismatch ($\sigma = 1, 50, 0.02$) and three values of the sample window size ($N = 15, 20, 25$). Since the sample window is not an input to the EKF, there are a total of 21 separate cases: 6 adaptive and 1 nonadaptive for each of the 3 noise mismatch values. In addition, a Monte Carlo simulation containing 10 realizations of the measurement noise process is performed for each of the 21 cases. The performance of the filters is then evaluated based on the mean and standard deviation of the miss distance distribution and on the average tracking error history.

The effect of the adaptive noise estimation can be seen in the tracking histories of the estimated variance for azimuth and elevation vs the actual variance. Figure 3 shows the typical behavior of the estimated azimuth measurement variance for $\sigma = 50$ and $N = 20$. The elevation profile is quite similar. Figure 4 shows the typical behavior of the estimated elevation measurement variance for $\sigma = 0.02$ and $N = 20$. The azimuth profile is quite similar. In Figs. 3 and 4 it can be seen how the estimated variance remains at the a priori value until the sample size of 20 is reached. Then, the filter begins using the value computed by the adaptive noise estimator. The estimates are then on the same order of magnitude as the actual variance. Near the terminal time, the actual variance begins to rise sharply and the estimates tend to lag behind. If the current measurement noise covariance matrix is found to be not positive definite, the last value of the estimate is used. This has happened on occasion during the last few sample times, probably because the negative terms in Eqs. (27) and (33) begin to dominate.

In testing the weighted limited-memory filter, only one value of β has been chosen in order to limit the number of parameters to be varied for filter comparison. The miss distance and the tracking error histories for $\beta = 3$, 4, 5, and 6

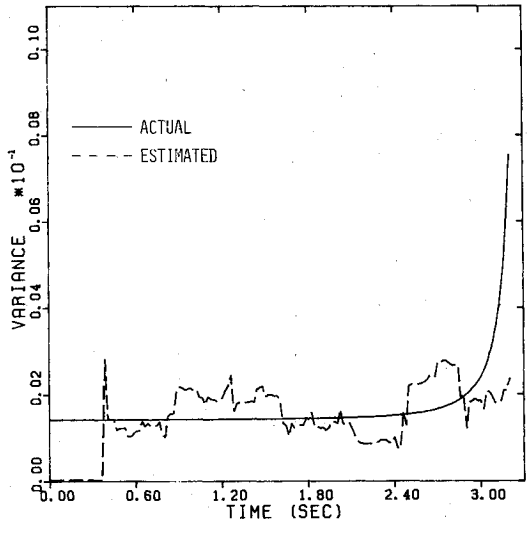

Fig. 3 Azimuth measurement variance estimate, $\sigma = 50$, $N = 20$.

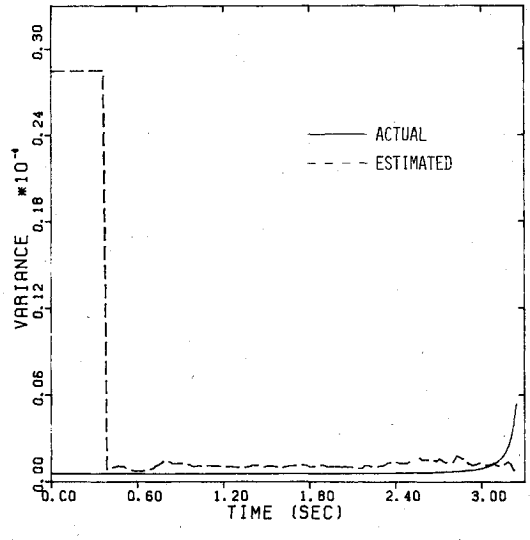

Fig. 4 Elevation measurement variance estimate, $\sigma = 0.02$, $N = 20$.

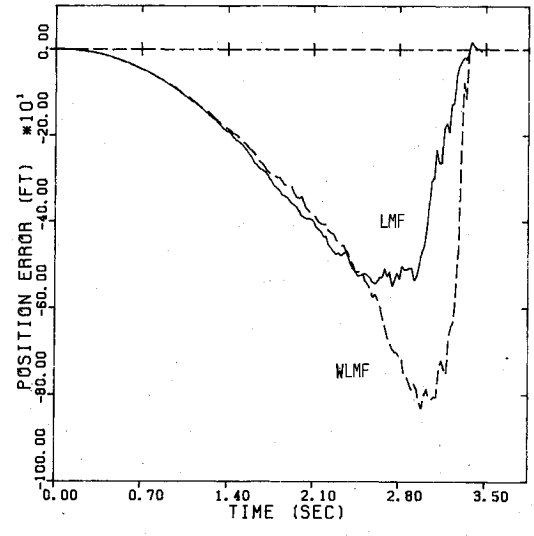

Fig. 5 Position error of adaptive filters, $\sigma = 50$, $N = 25$.

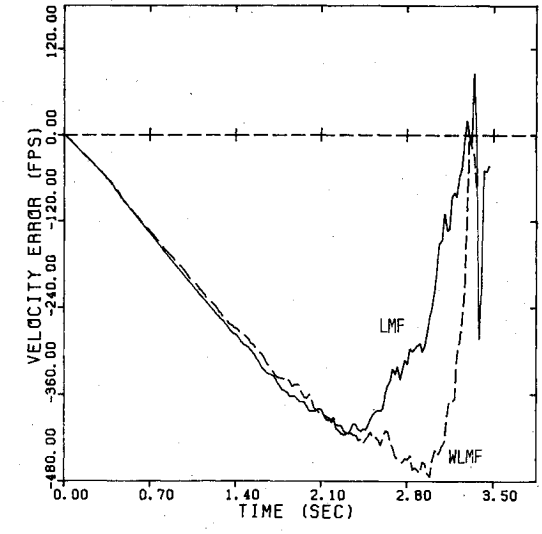

Fig. 6 Velocity error for adaptive filters, $\sigma = 50$, $N = 25$.

with $\sigma = 50$ and $N = 20$ have been evaluated to determine a value of β. Based on the results, $\beta = 5$ has been chosen. The weights generated by this value of β can be obtained by Eq. (29). The weight factor is zero at first and then increases during the run. Since the flight time for the launch scenario used in this study is approximately 4 s and the filter cycle time is 0.02 s, a total of about 200 samples is available.

The means and standard deviations of the miss distance distributions for the 21 cases are shown in Table 2. Clearly, the adaptive filters are performing better than the EKF. With regard to the two adaptive filters, the WLMF generally gives lower average miss distances than the LMF. However, there does not seem to be sufficient improvement to justify the additional computer storage and computation time required by the WLMF. Finally, the adaptive filters seem to be only mildly sensitive to the window size N, that is, the number of samples included in the estimation of the measurement noise covariance. However, since the average miss distance generally decreases as N increases, the tracking error histories have been generated with the value $N = 25$.

In this paper, the tracking error is defined as the difference between the true value and the estimated value. For example, the definition of position error is

$$\text{Position error} = (x_r^2 + y_r^2 + z_r^2)^{1/2} - (\hat{x}_r^2 + \hat{y}_r^2 + \hat{z}_r^2)^{1/2} \qquad (37)$$

Furthermore, the error histories presented here are the averages of 10 Monte Carlo runs, and the seed that initiates the noise sequence is the same from one set of runs to another.

For $\sigma = 1$, the tracking errors of the LMF and the WLMF are of the same order of magnitude as the EKF, which is expected since there is no noise mismatch.

A dramatic improvement in the tracking error by the adaptive filters occurs when $\sigma = 50$. Relative position, relative

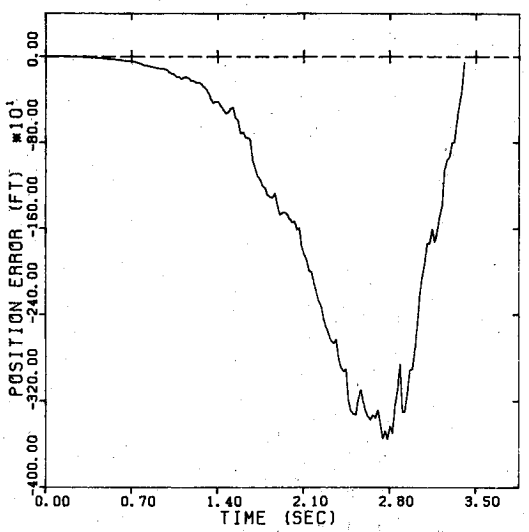

Fig. 8 Position error of the EKF, $\sigma = 50$.

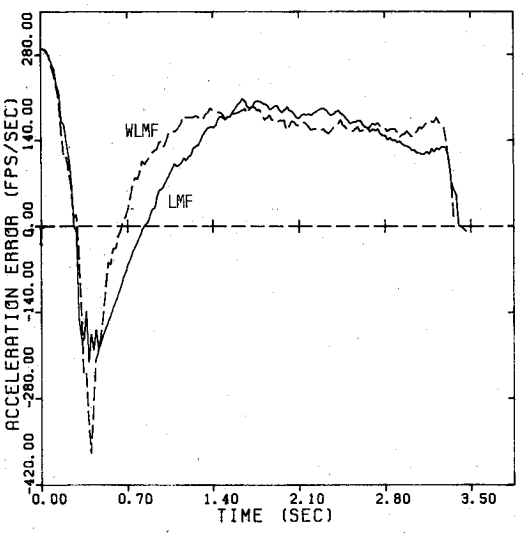

Fig. 7 Target acceleration error for adaptive filters, $\sigma = 50$, $N = 25$.

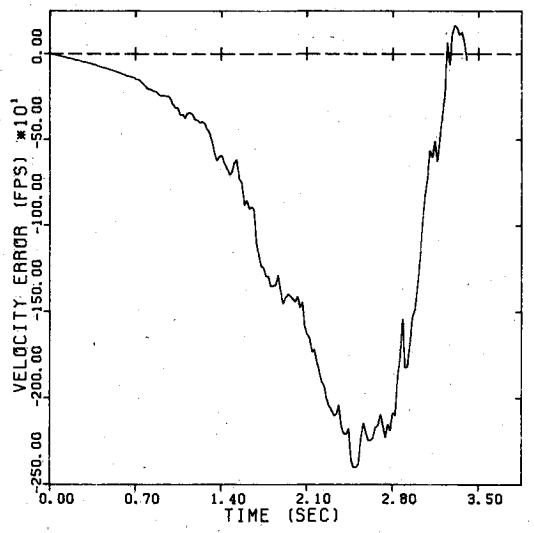

Fig. 9 Velocity error for EKF, $\sigma = 50$.

Table 2 Means and standard deviations of miss distance (ft) distributions

Filter	Mean	Standard deviation	$N=15$		$N=20$		$N=25$	
$\sigma=1$								
EKF	35.237	9.429						
LMF			18.843	4.248	10.516	5.172	8.781	4.788
WLMF			9.417	5.343	8.898	6.129	7.084	4.571
$\sigma=50$								
EKF	131.084	40.461						
LMF			66.993	26.391	67.384	28.697	67.374	30.098
WLMF			60.306	15.589	59.519	21.633	65.320	15.768
$\sigma=0.02$								
EKF	47.696	1.160						
LMF			3.014	1.729	2.639	1.319	2.583	1.268
WLMF			2.701	1.829	3.062	1.662	2.600	1.212

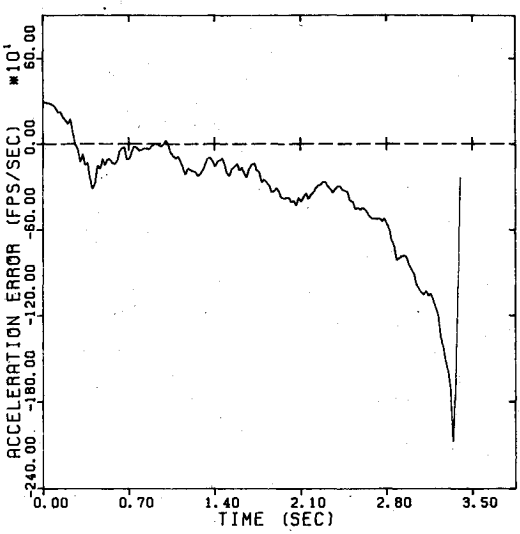

Fig. 10 Target acceleration error for EKF, $\sigma = 50$.

velocity, and target acceleration errors are presented in Figs. 5-10 for the adaptive filters and, for comparison, the EKF. While the maximum position error for the EKF is almost 4000 ft, the position errors of the adaptive filters are around 600 ft for the LMF and 800 ft for the WLMF (see Figs. 5 and 8). Velocity errors are shown in Figs. 6 and 9. It is seen that the maximum velocity error for the adaptive filters is less than 500 ft/s, while the same error for the EKF is nearly 2500 ft/s. Finally, the maximum target acceleration error for the EKF is around six times larger than that for the adaptive filters. Note that the LMF generally performs better than the WLMF.

For $\sigma = 0.02$, the tracking error histories are significantly different than those of the EKF, but they give little insight to the improved miss performance of the adaptive filters.

Conclusions

Adaptive schemes for measurement noise estimation in a homing missile guidance system have been investigated. The objective has been to implement these schemes in a missile intercept simulation and observe whether or not an improvement in tracking performance or miss distance can be achieved. The information contained in the measurement residual sequence has been incorporated into two algorithms that provide on-line estimates of the measurement noise variance to an extended Kalman filter. The test results indicate that improvement over the nonadaptive scheme is obtained.

The limited-memory noise estimator has demonstrated an ability to adapt in real time to the local noise environment. The estimator detects successfully the order of magnitude of the noise variance, regardless of the mismatch between the a priori value and the actual value. However, the algorithm has difficulty tracking the rapid change in the noise variance during the final stage.

The combination of the noise estimator and the extended Kalman filter is called the limited-memory filter. The adaptive feature of this filter can improve the state estimation process when the measurement noise is greater than expected, as in the cases where $\sigma = 50$. The weighted limited-memory filter also exhibits improved performance, most notably in the miss distance distributions of the cases where the measurement noise variance is less than the a priori value. It appears that some type of weighting scheme is helpful, but the one used here is not necessarily the best choice. One drawback is that the code for the weighted scheme requires approximately twice as much storage as the nonweighted adaptive scheme; however, the execution time is only slightly increased. The differences between the two adaptive filters could become more pronounced perhaps if a larger number of runs are included in the Monte Carlo simulations.

Acknowledgment

This research has been supported by the Air Force Armament Laboratory, Eglin AFB, under Contract FO8635-81-R-0211, managed by Capt. R.K. Liefer. The authors are also indebted to John R. Nolan for computational assistance.

References

[1] Jazwinski, A.H., *Stochastic Processes and Filtering Theory,* Academic Press, New York, 1970.

[2] Bryson, A.E. and Ho, Y.-C., *Applied Optimal Control,* Blaisdell, Waltham, Mass. 1969.

[3] Speyer, J.L. and Hull, D.G., "Comparison of Several Extended Kalman Formulations for Homing Missile Guidance," *Proceedings of AIAA Guidance and Control Conference,* AIAA, New York, 1980, pp. 392-398.

[4] Myers, K.A. and Tapley, B.D., "Adaptive Sequential Estimation with Unknown Noise Statistics," *IEEE Transactions on Automatic Control,* Vol. AC-21, No. 4, Aug. 1976, pp. 520-523.

[5] Smith, R.C., "A Six-Degree-of-Freedom Computer Simulation of an Air-to-Air Missile Intercept," M.S. Thesis, The University of Texas at Austin, May 1979.